Table 1. hTERT and human dyskerin peptides sequenced by nanoLC-MS/MS (*21*).

hTERT	Dyskerin
$_{202}$AWNHSVR$_{208}$	$_{292}$LLTSHKR$_{297}$
$_{1085}$HRVTYVPLLGSLR$_{1097}$	$_{378}$KWGLGPK$_{384}$
$_{143}$RVGDDVLVHLLAR$_{155}$	$_{400}$HGKPTDSTPATWK$_{412}$
$_{249}$TPVGQGSWAHPGR$_{261}$	$_{144}$SQQSAGKEYVGIVR$_{157}$
$_{552}$RSPGVGCVPAAEHR$_{535}$	$_{65}$TTHYTPLACGSNPLKR$_{80}$
$_{866}$LVDDFLLVTPHLTHAK$_{881}$	$_{394}$QGLLDKHGKPTDSTPATWK$_{412}$
$_{246}$PERTPVGQGSWAHPGR$_{261}$	$_{19}$KSLPEEDVAEIQHAEEFLIKPESK$_{42}$
$_{672}$RPGLLGASVLGLDDIHR$_{688}$	
$_{276}$ARPAEEATSLEGALSGTR$_{293}$	
$_{670}$ARRPGLLGASVLGLDDIHR$_{688}$	
$_{240}$RGAAPEPERTPVGQGSWAHPGR$_{261}$	

to associate with telomerase (table S1) may be involved in its biogenesis, trafficking, recruitment to the telomere, and degradation. However, from the analyses described here, it can be concluded that these proteins are not required for nucleotide addition, nor do they constitute integral components of the catalytically active enzyme complex.

References and Notes

1. R. K. Moyzis *et al.*, *Proc. Natl. Acad. Sci. U.S.A.* **85**, 6622 (1988).
2. C. B. Harley, A. B. Futcher, C. W. Greider, *Nature* **345**, 458 (1990).
3. A. M. Olovnikov, *J. Theor. Biol.* **41**, 181 (1973).
4. C. W. Greider, E. H. Blackburn, *Cell* **43**, 405 (1985).
5. J. Lingner *et al.*, *Science* **276**, 561 (1997).
6. T. M. Nakamura *et al.*, *Science* **277**, 955 (1997).
7. J. Feng *et al.*, *Science* **269**, 1236 (1995).
8. J. Lingner, T. R. Cech, *Proc. Natl. Acad. Sci. U.S.A.* **93**, 10712 (1996).
9. C. Wenz *et al.*, *EMBO J.* **20**, 3526 (2001).
10. G. Schnapp, H. Rodi, W. J. Rettig, A. Schnapp, K. Damm, *Nucleic Acids Res.* **26**, 3311 (1998).
11. Materials and methods are available as supporting material on *Science* Online.
12. G. Wallweber, S. Gryaznov, K. Pongracz, R. Pruzan, *Biochemistry* **42**, 589 (2003).
13. T. M. Bryan, A. Englezou, M. A. Dunham, R. R. Reddel, *Exp. Cell Res.* **239**, 370 (1998).
14. N. S. Heiss *et al.*, *Nat. Genet.* **19**, 32 (1998).
15. J. R. Mitchell, J. Cheng, K. Collins, *Mol. Cell. Biol.* **19**, 567 (1999).
16. J. R. Mitchell, E. Wood, K. Collins, *Nature* **402**, 551 (1999).
17. M. Armanios *et al.*, *Proc. Natl. Acad. Sci. U.S.A.* **102**, 15960 (2005).
18. T. Vulliamy *et al.*, *Nature* **413**, 432 (2001).
19. T. L. Beattie, W. Zhou, M. O. Robinson, L. Harrington, *Mol. Cell. Biol.* **21**, 6151 (2001).
20. K. Arai *et al.*, *J. Biol. Chem.* **277**, 8538 (2002).
21. Single-letter abbreviations for the amino acid residues are as follows: A, Ala; C, Cys; D, Asp; E, Glu; F, Phe; G, Gly; H, His; I, Ile; K, Lys; L, Leu; M, Met; N, Asn; P, Pro; Q, Gln; R, Arg; S, Ser; T, Thr; V, Val; W, Trp; and Y, Tyr.

22. We thank the laboratory of T. Bryan (Cell Biology Unit, Children's Medical Research Institute) for assistance with telomerase methods and L. Cheong, L. Lu, and T. Phan (Commonwealth Scientific and Industrial Research Organisation) for fermentation support. This research was supported by the Carcinogenesis Fellowship of the Cancer Council of New South Wales and by the National Health and Medical Research Council of Australia. The accession numbers for hTERT and human dyskerin are O14746 and CAA11970, respectively.

Supporting Online Material

www.sciencemag.org/cgi/content/full/315/5820/1850/DC1
Materials and Methods
Figs. S1 to S5
References

8 December 2006; accepted 27 February 2007
10.1126/science.1138596

Regulation of Hepatic Stellate Cell Differentiation by the Neurotrophin Receptor p75^{NTR}

Melissa A. Passino, Ryan A. Adams, Shoana L. Sikorski, Katerina Akassoglou*

Differentiation of hepatic stellate cells (HSCs) to extracellular matrix– and growth factor–producing cells supports liver regeneration through promotion of hepatocyte proliferation. We show that the neurotrophin receptor p75^{NTR}, a tumor necrosis factor receptor superfamily member expressed in HSCs after fibrotic and cirrhotic liver injury in humans, is a regulator of liver repair. In mice, depletion of p75^{NTR} exacerbated liver pathology and inhibited hepatocyte proliferation in vivo. *p75$^{NTR-/-}$* HSCs failed to differentiate to myofibroblasts and did not support hepatocyte proliferation. Moreover, inhibition of p75^{NTR} signaling to the small guanosine triphosphatase Rho resulted in impaired HSC differentiation. Our results identify signaling from p75^{NTR} to Rho as a mechanism for the regulation of HSC differentiation to regeneration-promoting cells that support hepatocyte proliferation in the diseased liver.

Liver regeneration driven by hepatocyte proliferation is necessary for tissue repair and survival after acute liver injury, liver transplantation, and chronic hepatic disease, such as liver fibrosis and cirrhosis (*1*). Induction of hepatocyte proliferation depends on cross-talk between hepatocytes and nonparenchymal liver cells, such as hepatic stellate cells (HSCs) (*1*). At sites of injury, HSCs differentiate to myofibroblasts and secrete extracellular matrix (ECM) and growth factors that support hepatocyte proliferation (*2*). Although HSC differentiation is considered a central process for the induction of liver regeneration, the molecular mechanisms that regulate the transition to repair-supporting cells in the liver remain poorly understood. Expression of p75^{NTR} is increased in HSCs in the cirrhotic liver in humans and in animal models (*3*, *4*). p75^{NTR} is expressed in the nervous system during development or after injury (*5*), and it has been primarily studied as a regulator of survival and apoptosis in neurons and glia cells (*6*). p75^{NTR} is also widely expressed in nonneuronal tissues (*7*). However, the biological importance of the injury-induced, nonneuronal expression of p75^{NTR} remains enigmatic.

To address the role of p75^{NTR} in liver disease in vivo, we crossed mice deficient for p75^{NTR} with plasminogen-deficient (*plg$^{-/-}$*) mice (*8*) that spontaneously develop liver disease (*9*, *10*). At 5 weeks of age, *plg$^{-/-}$p75$^{NTR-/-}$* mice were smaller than littermate controls (fig. S1A). *plg$^{-/-}$* mice have a median survival time of 6 months (*10*). By contrast, *plg$^{-/-}$p75$^{NTR-/-}$* mice had a median survival time of 2.5 months (Fig. 1A). *plg$^{-/-}$p75$^{NTR-/-}$* mice showed prominent liver lesions as early as 10 weeks of age (fig. S1B), with large necrotic areas (Fig. 1B) not observed in either wild-type (WT) or 10-week-old *plg$^{-/-}$* control littermates. Overall, these results suggest that p75^{NTR} plays a protective role in liver disease.

We hypothesized that p75^{NTR} might regulate the progression of liver disease via altering the pathophysiological characteristics of HSCs. WT control mice expressed low amounts of p75^{NTR},

Department of Pharmacology, University of California, San Diego (UCSD), La Jolla, CA 92093–0636, USA.

*To whom correspondence should be addressed. E-mail: akass@ucsd.edu

whereas livers of $plg^{-/-}$ mice expressed more $p75^{NTR}$ (Fig. 2A), which colocalized with the HSC marker desmin (Fig. 2B). Gene expression of both α-smooth muscle actin (*αSMA*) and collagen I (*col1α1*), which are expressed by HSCs after differentiation to myofibroblasts (*11*), was significantly reduced in the livers of $plg^{-/-}p75^{NTR-/-}$ mice compared with that in the livers of $plg^{-/-}$ mice (Fig. 2C). Total numbers of HSCs were similar between $plg^{-/-}$ and $plg^{-/-}p75^{NTR-/-}$ mice (fig. S6C). Examination of fibrin deposition, which is the causative agent for liver disease in the $plg^{-/-}$ mouse (*10*), showed no differences between $plg^{-/-}$ and $plg^{-/-}p75^{NTR-/-}$ mice (fig. S2). Overall, these results suggest that $p75^{NTR}$ regulates liver pathology by inducing HSC activation.

To examine whether $p75^{NTR}$ might directly regulate HSC differentiation to myofibroblasts, we assessed the ability of primary HSCs isolated from $p75^{NTR-/-}$ mice to differentiate in vitro. WT HSCs undergo activation within 2 weeks in culture, and $p75^{NTR}$ expression positively correlates with HSC activation (*4*). After 3 weeks in culture, WT HSCs exhibited morphologic features of activated myofibroblasts, whereas $p75^{NTR-/-}$ HSCs were mostly in a quiescent state (Fig. 3A). $p75^{NTR-/-}$ HSCs showed significantly reduced differentiation (fig. S3A) and reduction in protein expression of αSMA and collagen I (fig. S3B), as well as reduced gene expression of both *col1α1* and transforming growth factor β–1 (*TGFβ-1*) (fig. S3C), compared with those of WT HSCs. Lentiviral short hairpin RNA–mediated knockdown of $p75^{NTR}$ in WT HSCs decreased cell differentiation compared with control (fig. S4, $P < 0.009$). Adenoviral delivery of $p75^{NTR}$ (*12*) in $p75^{NTR-/-}$ HSCs restored differentiation (Fig. 3B).

The effects of $p75^{NTR}$ on HSC differentiation occurred in the absence of exogenous neurotrophin ligands. $p75^{NTR}$ contributes to several signaling pathways and biological functions, not only following neurotrophin binding but also independently of neurotrophins (*5*, *13*–*15*). In the absence of neurotrophins, $p75^{NTR}$ or the intracellular domain (ICD) of $p75^{NTR}$ alone can induce apoptosis (*16*, *17*) and activation of phosphatidylinositol 3-kinase (*12*) and Rho (*18*). Moreover, $p75^{NTR}$ may act in combination with other receptors, such as Nogo receptor, to mediate biological effects (*5*, *14*, *19*). Neutralization of neurotrophins either by antibody to nerve growth factor (NGF), neurotrophin scavenger Fc-$p75^{NTR}$, or brain-derived neurotrophic factor (BDNF) scavenger Fc-TrkB, or inhibition of the other neurotrophin receptor, Trk, had no effect on HSC differentiation (fig. S5). Adenoviral delivery of the ICD of $p75^{NTR}$ restored differentiation of the $p75^{NTR-/-}$ HSCs to an extent similar to that of full-length (FL) $p75^{NTR}$ (Fig. 3B). Prior studies have shown a 1.5-fold increase in HSC apoptosis after exposure to exogenous NGF (*4*), which we confirmed (fig. S6A). Our differentiation experiments (Fig. 3 and figs. S3 to S5 and S7) were done in the absence of exogenous NGF, and WT and $p75^{NTR-/-}$ HSCs showed no difference in apoptosis (fig. S6A), suggesting that apoptosis cannot account for the differences observed in HSC differentiation. HSCs do not show apoptosis in 10-week-old $plg^{-/-}$ mice, whereas apoptosis in the livers of $plg^{-/-}p75^{NTR-/-}$ mice was exclusive to hepatocytes (fig. S6B). These results confirm data from human liver fibrotic disease showing that HSC apoptosis occurs primarily at late stages of liver disease (*20*) and that differentiated HSCs are resistant to apoptosis (*21*). The number of total desmin-positive HSCs was similar in adult WT and $p75^{NTR-/-}$ mice, suggesting that $p75^{NTR}$ does not affect the developmental differentiation or the total number of HSCs (fig. S6C).

The signal transduction mechanisms that promote and control HSC differentiation into myofibroblasts remain elusive. Rho is implicated in regulating myofibroblast morphology through reorganization of the actin cytoskeleton (*22*). A signaling relationship between $p75^{NTR}$ and Rho is well documented in the nervous system, where $p75^{NTR}$-mediated Rho signaling is involved in the regulation of neurite outgrowth (*23*). Because either $p75^{NTR}$ in the absence of ligand or the ICD of $p75^{NTR}$ alone can activate Rho through a direct interaction (*18*) and because Rho is involved in promoting the myofibroblastic state of HSCs (*22*), we examined whether $p75^{NTR}$ promoted HSC activation through Rho. Unlike in WT HSCs, expression of phospho-cofilin, a marker for Rho activation (*24*), was undetectable in $p75^{NTR-/-}$ HSCs (Fig. 3C). Adenoviral delivery of constitutively activated Rho (*25*) restored differentiation in $p75^{NTR-/-}$ HSCs (Fig. 3D). WT HSCs treated with TAT-Pep5, which is a cell-permeable peptide inhibitor that specifically blocks the activation of Rho through $p75^{NTR}$ (*23*), showed undifferentiated morphology (Fig. 3E), reduced immunostaining of phospho-cofilin (fig. S7A), and decreased gene expression of *col1α1* and *TGFβ-1* (fig. S7B), similar to the features of $p75^{NTR-/-}$ HSCs. Taken together, these results suggest that $p75^{NTR}$ signaling through Rho promotes HSC differentiation to myofibroblasts.

Because cross-talk of HSCs with hepatocytes drives hepatocyte proliferation and liver repair

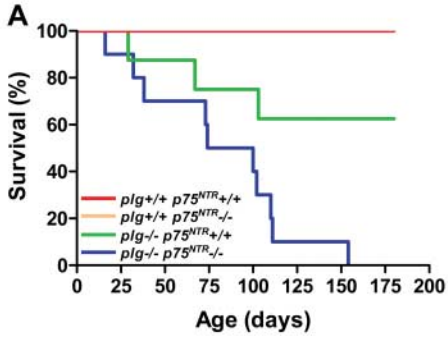

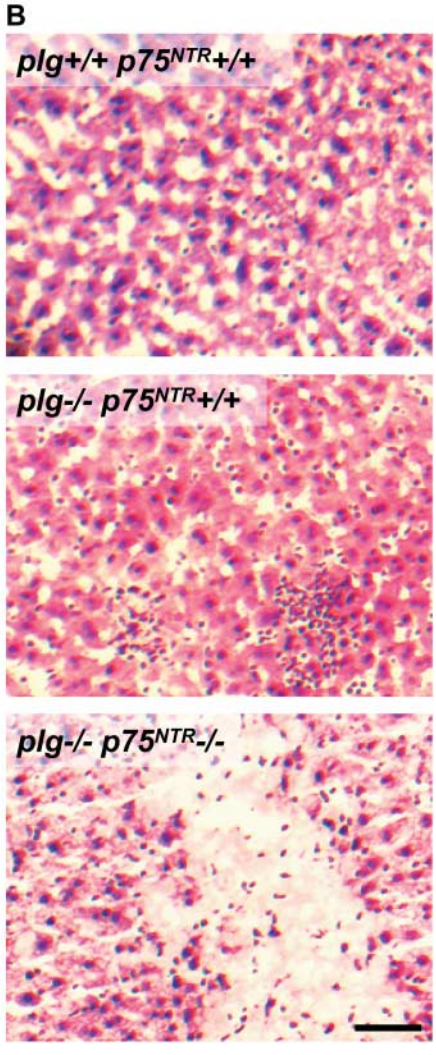

Fig. 1. Exacerbated mortality and liver pathology caused by $p75^{NTR}$ deficiency. (**A**) Survival of $plg^{+/+}p75^{NTR+/+}$ ($n = 35$), $plg^{+/+}p75^{NTR-/-}$ ($n = 11$), $plg^{-/-}p75^{NTR+/+}$ ($n = 8$), and $plg^{-/-}p75^{NTR-/-}$ ($n = 10$) mice. Because both $plg^{+/+}p75^{NTR+/+}$ and $plg^{+/+}p75^{NTR-/-}$ mice exhibited 100% survival, the curves overlap and appear as a single line. (**B**) Hematoxylin stain of representative liver sections of 10-week-old $plg^{+/+}p75^{NTR+/+}$ (top), $plg^{-/-}p75^{NTR+/+}$ (middle), and $plg^{-/-}p75^{NTR-/-}$ (bottom) mice. Scale bar indicates 56 μm.

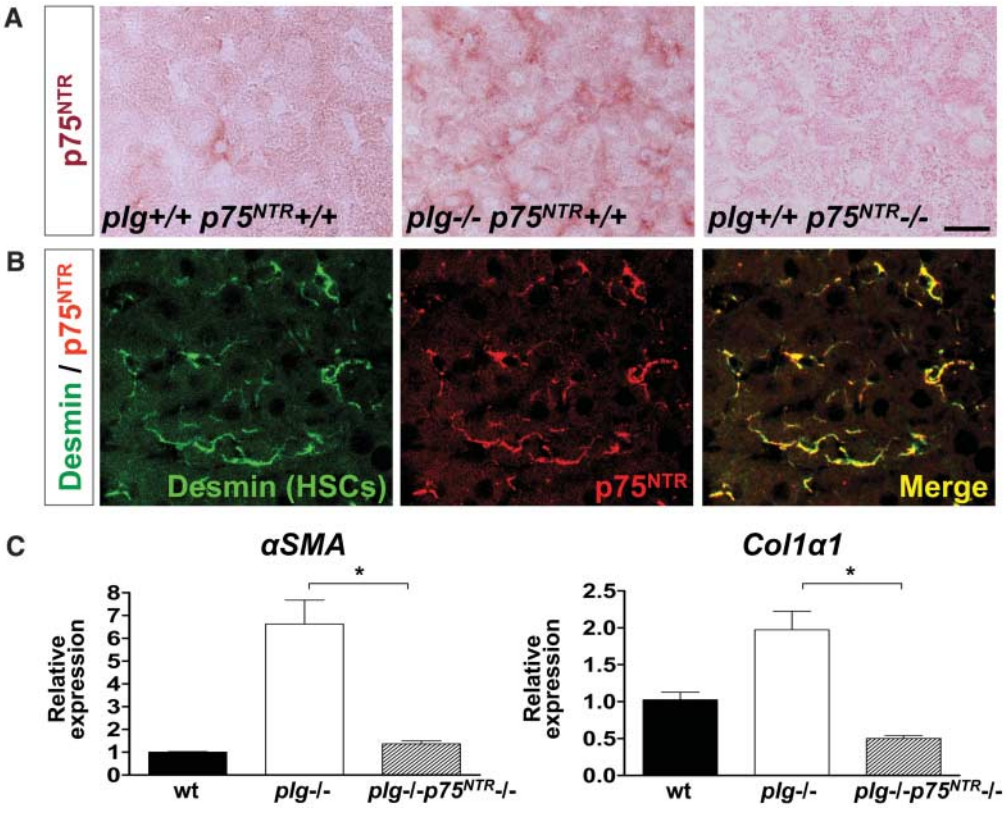

Fig. 2. Inhibited HSC activation after loss of $p75^{NTR}$. (**A**) Immunochemical detection of $p75^{NTR}$ (dark red) in livers of 10-week-old $plg^{+/+}p75^{NTR+/+}$ (left), $plg^{-/-}p75^{NTR+/+}$ (middle), and $plg^{+/+}p75^{NTR-/-}$ (right; negative control) mice. Immunoreactive cells show spindle morphology and perihepatocyte localization characteristic of HSCs. (**B**) Confocal double immunofluorescence in $plg^{-/-}$ liver shows colocalization (yellow) of the HSC marker desmin (green) with $p75^{NTR}$ (red). (**C**) Analysis of markers of HSC activation in whole liver. *αSMA* and *col1α1* gene expression was examined in 4-week-old mice (n = 3 mice per genotype) by real-time polymerase chain reaction (PCR) analysis performed in duplicates. Bar graphs represent means ± SEM [*P < 0.001 by one-way analysis of variance (ANOVA)]. Scale bar shown can be applied to all images and represents 19 μm in (A) and 25 μm in (B).

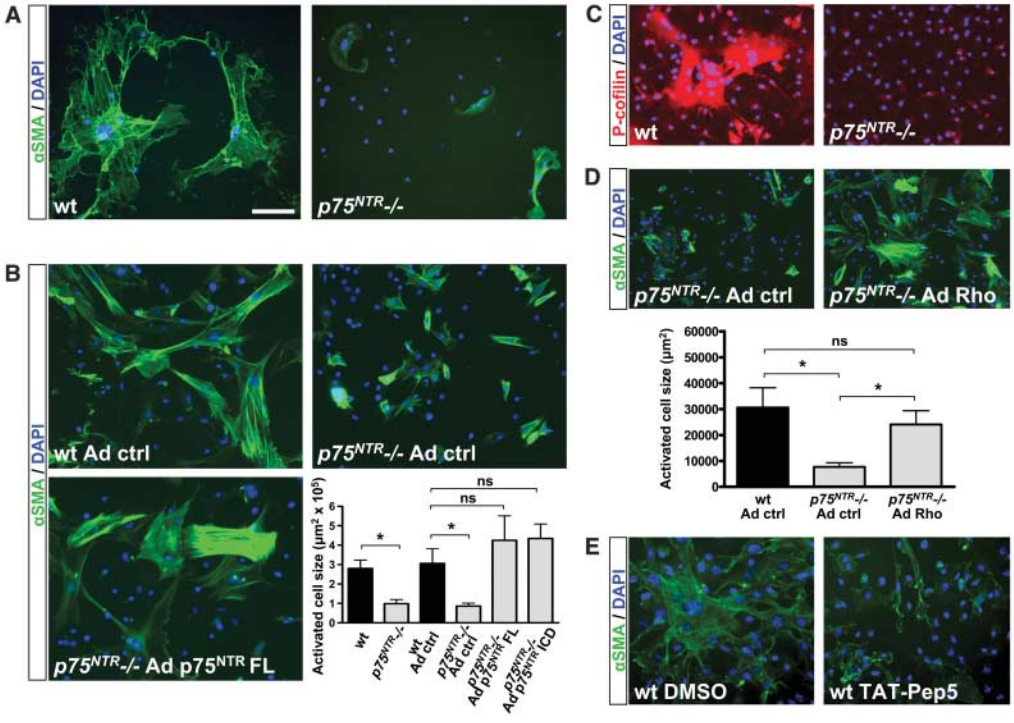

Fig. 3. Role of Rho in $p75^{NTR}$-promoted HSC activation. (**A**) αSMA immunostaining (green) of activated WT and $p75^{NTR-/-}$ HSCs after 21 days in culture. Wt HSCs are characterized by wide, spread-out morphology and large round nuclei. $p75^{NTR-/-}$ HSCs are unable to differentiate, and the few cells that showed immunostaining for αSMA are arrested at an intermediate stage of differentiation, characterized by small size and shrunken morphology. Nuclei are stained with 4′,6′-diamidino-2-phenylindole (DAPI) (blue). Representative images from seven independent experiments are shown. (**B**) Adenoviral delivery of FL or ICD $p75^{NTR}$. Freshly isolated WT and $p75^{NTR-/-}$ HSCs were transduced on day 2 with adenovirus. αSMA immunostaining (green) was performed on day 7. Nuclei were stained with DAPI (blue). Activated cell size was quantitated by determining the area of αSMA-positive cells in three independent experiments performed in duplicates. Adenoviral empty vector was used as control (Ad ctrl). Bar graphs represent means ± SEM (*P < 0.05 and ns, not significant, by one-way ANOVA). (**C**) Detection of phosphorylated cofilin (P-cofilin), a marker indicative of Rho activation, by immunostaining (red) in WT and $p75^{NTR-/-}$ HSCs after 21 days in culture. Nuclei are stained with DAPI (blue). (**D**) Adenoviral delivery of constitutively active Rho. HSC transduction and analysis of activated cell size was done as described in (B). Bar graphs represent means ± SEM (*P < 0.05 and ns, not significant, by one-way ANOVA). (**E**) Specific blocking of $p75^{NTR}$-mediated Rho activation. Representative images of αSMA immunostaining (green) of freshly isolated WT HSCs after a 7-day treatment with either vehicle [dimethyl sulfoxide (DMSO)] or TAT-Pep5. TAT-Pep5 is a fused peptide of the amino-terminal protein transduction domain (11 amino acids) from the human immunodeficiency virus protein TAT with Pep5, which is a peptide inhibitor of the activation of Rho by $p75^{NTR}$. Nuclei are stained with DAPI (blue). Scale bar shown can be applied to all images and represents 93 μm in (A), 79 μm in (B), 93 μm in (C), 105 μm in (D), and 32 μm in (E).

(*1*, *2*, *26*), we examined whether p75^{NTR} could regulate hepatocyte proliferation. *plg*$^{-/-}$ mice showed an increased number of proliferating hepatocytes [126.6 ± 3.9 (SEM), Fig. 4A] when compared with WT mice [95.2 ± 3.7 (SEM)], suggestive of the regenerative response in the liver after injury. By contrast, *plg*$^{-/-}$*p75*$^{NTR-/-}$ mice displayed significantly decreased cell proliferation [74.2 ± 9.1 (SEM)] compared with *plg*$^{-/-}$ mice (Fig. 4A, $P < 0.001$). One of the key mediators in promoting hepatocyte proliferation is hepatocyte growth factor (HGF) (*1*). Whole-liver homogenates from *plg*$^{-/-}$*p75*$^{NTR-/-}$ mice showed only one-third of the amount of HGF protein detected in *plg*$^{-/-}$ livers (Fig. 4B). HSCs are a major source of HGF in the liver (*27*, *28*); thus, the reduction in HGF in the *plg*$^{-/-}$*p75*$^{NTR-/-}$ mouse is in accordance with the defective HSC activation observed after genetic loss of p75^{NTR} both in vivo (Fig. 2C) and in vitro (Fig. 3). In co-culture (*26*), hepatocytes in culture with *p75*$^{NTR-/-}$ HSCs exhibited a 30% decrease in proliferation compared with those incubated with WT HSCs (Fig. 4C, $P < 0.05$). Proliferation was largely restored when HGF was added to the culture medium (Fig. 4C). Taken together, these results suggest that p75^{NTR} expression by HSCs is necessary for their differentiation to repair-supporting, HGF-secreting cells, which in turn can promote hepatocyte proliferation.

HSC differentiation is a hallmark of fibrotic liver disease of different etiologies, such as hepatitis and chronic alcohol consumption (*20*). Initiation of HSC differentiation results in secretion of HGF and synthesis of ECM, which are critical mediators for the restoration of normal liver structure, hepatocyte proliferation, and liver regeneration (*1*). However, perpetuation of HSC activation to a myofibroblastic state leads to excessive collagen and ECM deposition, which results in liver fibrosis. Therefore, sustained differentiation of HSCs is considered a target for the treatment of liver fibrosis (*11*). At late stages of liver disease, resolution of fibrosis depends on HSC apoptosis (*20*). Our study showed that p75^{NTR} induces HSC differentiation and demonstrated that the mild in vitro effect of NGF on HSC apoptosis (*4*, *29*) is mediated by p75^{NTR}. These results suggest that in liver injury p75^{NTR} might function both as a regulator of HSC differentiation and, depending on the bioavailability of neurotrophins, might also participate together with other apoptotic mediators in orchestrating the resolution of fibrosis. Identification of p75^{NTR} as a molecular link between HSC activation and hepatocyte proliferation could provide a therapeutic target for manipulating the stages of HSC activation during the progression of chronic liver disease.

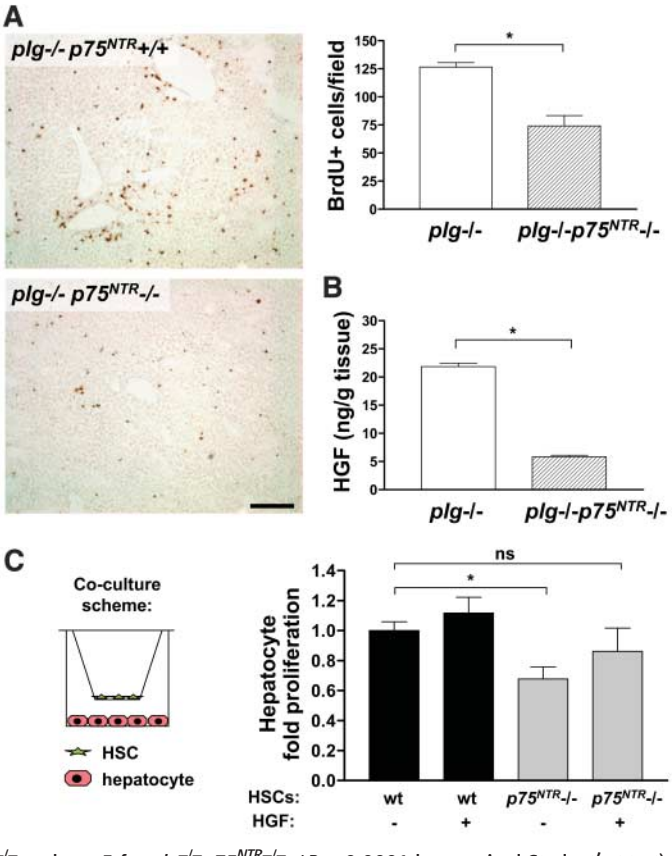

Fig. 4. p75^{NTR}-dependent promotion of hepatocyte proliferation through regulation of HGF secretion by HSCs. (**A**) Liver cell proliferation in *plg*$^{-/-}$*p75*$^{NTR+/+}$ and *plg*$^{-/-}$*p75*$^{NTR-/-}$ mice. Ten-week-old mice were injected intraperitoneally with bromodeoxyuridine (BrdU) (100 mg/kg) daily for 3 days. Proliferating cells were visualized by immunochemical detection of BrdU. Liver cell proliferation was quantified by counting the number of BrdU+ cells per field (field corresponds to 1.5 mm^2) (top right). Graph represents mean ± SEM ($n = 5$ per genotype, $^*P < 0.001$ by unpaired Student's t test). Scale bar, 198 μm. (**B**) HGF in the livers of *plg*$^{-/-}$ and *plg*$^{-/-}$*p75*$^{NTR-/-}$ mice as quantified by enzyme-linked immunosorbent assay. Graph represents mean ± SEM ($n = 8$ for *plg*$^{-/-}$ and $n = 5$ for *plg*$^{-/-}$*p75*$^{NTR-/-}$, $^*P < 0.0001$ by unpaired Student's t test). (**C**) Culture of primary hepatocytes with WT and *p75*$^{NTR-/-}$ HSCs. Hepatocytes were plated in the bottom of the well and incubated with HSCs grown on inserts placed within the well. Hepatocytes were cultured with WT or *p75*$^{NTR-/-}$ HSCs (day 7 to 21, passage 2 to 4), with or without HGF (50 ng/ml). After 2 days, hepatocyte proliferation was assessed by [^{3}H]thymidine incorporation (right). All data are mean ± SEM from four independent experiments performed in duplicates ($^*P < 0.05$ and ns, not significant, by one-way ANOVA).

References and Notes

1. R. Taub, *Nat. Rev. Mol. Cell Biol.* **5**, 836 (2004).
2. C. Balabaud, P. Bioulac-Sage, A. Desmouliere, *J. Hepatol.* **40**, 1023 (2004).
3. D. Cassiman, C. Denef, V. J. Desmet, T. Roskams, *Hepatology* **33**, 148 (2001).
4. N. Trim *et al.*, *Am. J. Pathol.* **156**, 1235 (2000).
5. M. V. Chao, *Nat. Rev. Neurosci.* **4**, 299 (2003).
6. G. Dechant, Y. A. Barde, *Nat. Neurosci.* **5**, 1131 (2002).
7. C. Lomen-Hoerth, E. M. Shooter, *J. Neurochem.* **64**, 1780 (1995).
8. Materials and methods are available on *Science* Online.
9. V. L. Ng *et al.*, *J. Hepatol.* **35**, 781 (2001).
10. T. H. Bugge *et al.*, *Cell* **87**, 709 (1996).
11. R. Bataller, D. A. Brenner, *Semin. Liver Dis.* **21**, 437 (2001).
12. P. P. Roux, A. L. Bhakar, T. E. Kennedy, P. A. Barker, *J. Biol. Chem.* **276**, 23097 (2001).
13. N. Zampieri, M. V. Chao, *Biochem. Soc. Trans.* **34**, 607 (2006).
14. P. A. Barker, *Neuron* **42**, 529 (2004).
15. K. K. Teng, B. L. Hempstead, *Cell. Mol. Life Sci.* **61**, 35 (2004).
16. S. Rabizadeh *et al.*, *Science* **261**, 345 (1993).
17. M. Majdan *et al.*, *J. Neurosci.* **17**, 6988 (1997).
18. T. Yamashita, K. L. Tucker, Y. A. Barde, *Neuron* **24**, 585 (1999).
19. L. F. Reichardt, *Philos. Trans. R. Soc. London Ser. B* **361**, 1545 (2006).
20. T. Kisseleva, D. A. Brenner, *J. Gastroenterol. Hepatol.* **21** (suppl. 3), S84 (2006).
21. E. Novo *et al.*, *Gut* **55**, 1174 (2006).
22. M. Kato *et al.*, *J. Hepatol.* **31**, 91 (1999).
23. T. Yamashita, M. Tohyama, *Nat. Neurosci.* **6**, 461 (2003).
24. M. Maekawa *et al.*, *Science* **285**, 895 (1999).
25. M. Hoshijima, V. P. Sah, Y. Wang, K. R. Chien, J. H. Brown, *J. Biol. Chem.* **273**, 7725 (1998).
26. N. Uyama *et al.*, *J. Hepatol.* **36**, 590 (2002).
27. Z. Hu, R. P. Evarts, K. Fujio, E. R. Marsden, S. S. Thorgeirsson, *Am. J. Pathol.* **142**, 1823 (1993).
28. J. J. Maher, *J. Clin. Investig.* **91**, 2244 (1993).
29. F. Oakley *et al.*, *Am. J. Pathol.* **163**, 1849 (2003).

30. We thank P. Barker and M. V. Chao for providing us with the p75^{NTR} adenoviral vectors and the p75^{NTR} antibodies, respectively, invaluable discussions, and critical reading of the manuscript; J. Heller Brown for the constitutive active adenoviral Rho vector; J. Han and T. Nuriel for technical assistance; members of P. Insel's lab for assistance with real-time polymerase chain reaction (PCR) and αSMA immunostaining protocol; W. Naugler for primary hepatocyte culture protocols; R. Rippe for HSC culture protocols; and K. Barrett for critical reading of the manuscript. Supported by NIH/National Institute of Neurological Disorders and Stroke (NINDS) grant P30-NS047101 to the UCSD Neuroscience Microscopy Shared Facility, NIH training grant 5T32-GM07752 to M.A.P., and NIH/NINDS grant NS051470 to K.A.

Supporting Online Material

www.sciencemag.org/cgi/content/full/315/5820/1853/DC1
Materials and Methods
Figs. S1 to S7
References

15 November 2006; accepted 28 February 2007
10.1126/science.1137603

Regulation of Hepatic Stellate Cell Differentiation by the Neurotrophin Receptor p75 NTR

Melissa A. Passino, Ryan A. Adams, Shoana L. Sikorski and Katerina Akassoglou (March 30, 2007)

Science **315** (5820), 1853-1856. [doi: 10.1126/science.1137603]

Editor's Summary

Science (print ISSN 0036-8075; online ISSN 1095-9203) is published weekly, except the last week in December, by the American Association for the Advancement of Science, 1200 New York Avenue NW, Washington, DC 20005.